https://doi.org/10.1109/LAWP.2008.2010566

Design of Decoupling Networks for Circulant Symmetric Antenna Arrays

Jacob C. Coetzee and Yantao Yu

Abstract— **Small element spacing in compact arrays results in strong mutual coupling between array elements. Performance degradation associated with the strong coupling can be avoided through the introduction of a decoupling network consisting of interconnected reactive elements. We present a systematic design procedure for decoupling networks of symmetrical arrays with more than three elements and characterized by circulant scattering parameter matrices. The elements of the decoupling network are obtained through repeated decoupling of the characteristic eigenmodes of the array, which allows the calculation of element values using closed-form expressions.**

Index Terms— **antenna arrays, antenna array feeds, adaptive arrays, mutual coupling**

I. Introduction

IN wireless systems such as mobile, personal communications, and wireless PBX/LAN networks, the use of multiple antennas can result in a significant increase in system capacity. With 2 or 3 antennas, the capacity of a mobile radio system can be doubled, while a 7-fold capacity increase can be achieved with 5 antennas [1]. Antenna diversity and MIMO can also provide improvements in quality and coverage. Multiport antennas usually have the design goal of isolated ports and uncorrelated radiation patterns. The effects of mutual coupling are usually contained by allowing for sufficient inter-element spacing. For spatial diversity on small platforms (e.g. mobile applications), employing an element spacing considerably smaller than the conventional half-wavelength spacing becomes inevitable. The increased mutual coupling apparently does not affect the capacity of a MIMO system [2], but it will decrease the antenna gain considerably and thus cause significant system performance degradation [3, 4].

A potential remedy is to introduce passive and lossless decoupling and matching networks. The decoupling network comprises of interconnected reactive elements and/or transmission line sections and stubs. It provides an additional signal path between the array elements, which effectively cancels the external coupling between them. The decoupling network for an *N*-port array is a 2*N*-port network with *N* ports connected to the array elements, while the remaining *N* ports represent the isolated input ports. Various implementations of decoupling networks have been described in the literature [5]-[10]. An alternative approach to achieve port decoupling involves the use of a modal feed network, where isolation between the new input ports is achieved by exploiting the inherent orthogonality of the eigenmodes of the array [11]-[14]. Although this approach is theoretically applicable to larger arrays, reported implementations of decoupling networks have been limited to a maximum of three or four radiators.

For maximum versatility, the number of elements in an adaptive array needs to be as large as possible. In this paper, the design of decoupling networks for symmetrical arrays with more than three elements and characterized by circulant scattering parameter matrices is explored. A systematic design approach which involves the repeated decoupling of the characteristic eigenmodes of the array is described. The procedure is illustrated by considering the example of a 6-element monopole array.

II. Basic Circuit Model

The circuit topologies to be used for the decoupling of two distinct eigenmodes will reduce to equivalent circuits resembling those shown in Fig. 1, where n_1 and n_2 are parameters which depend on the topology and the eigenmodes under consideration. The circuits in Fig. 1 are terminated in impedances $Z_1 = R_1 + jX_1$ and $Z_2 = R_2 + jX_2$. A series element of impedance of jX and parallel elements with admittances of jn_1B and jn_2B are used to transform Z_1 and Z_2 to produce input admittances of Y_1' and Y_2'. The input admittances are given by

$$Y_1' = \left(Z_1 + jX\right)^{-1} + jn_1B,$$
$$Y_2' = \left(Z_2 + jX\right)^{-1} + jn_2B. \tag{1}$$

Given n_1 and n_2, the aim is calculate values for X and B which will match the input admittances. Setting $Y_1' = Y_2'$ and evaluating the real and imaginary parts give

$$X = g(Z_1, Z_2) = \frac{-b \pm \sqrt{b^2 - 4ac}}{2a}, \tag{2}$$

and

$$B = h(Z_1, n_1, Z_2, n_2, X) = \frac{1}{(n_1 - n_2)}\left(\frac{X_1 + X}{R_1^2 + \left(X_1 + X\right)^2} - \frac{X_2 + X}{R_2^2 + \left(X_2 + X\right)^2}\right), \tag{3}$$

Manuscript received October 14, 2008.

J. C. Coetzee is with the School of Engineering Systems, Queensland University of Technology, GPO Box 2434, Brisbane, QLD 4001, Australia (e-mail: j.coetzee@qut.edu.au).

Y. Yu is with the Department of Electrical and Computer Engineering, National University of Singapore, Singapore, 117576 (e-mail: yantaoyu@nus.edu.sg).

where $a = R_1 - R_2$, $b = 2\left(R_1 X_2 - R_2 X_1\right)$ and $c = R_1\left(R_2^{\,2} + X_2^{\,2}\right) - R_2\left(R_1^{\,2} + X_1^{\,2}\right)$. These expressions can be used to design a decoupling network for a larger array.

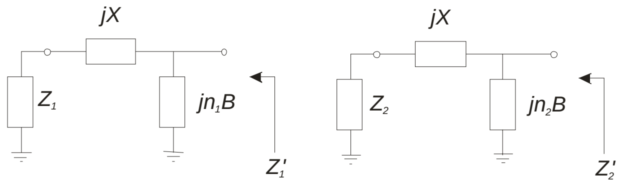

Fig. 1. General circuit model for matching two distinct terminating impedances.

III. DECOUPLING OF LARGER ARRAYS

Decoupling of an array involves a process of modifying its impedance matrix to reduce all the off-diagonal elements to zero. For arrays characterized by circulant scattering parameter matices, decoupling can also be regarded as a process of equalizing the eigenmode impedances (i.e. the eigenvalues of the impedance matrix). The corresponding orthogonal eigenvectors can be viewed as the port voltages under the conditions when a specific mode is excited.

Using our approach, an *N*-element array characterized by a circulant impedance matrix with *k* distinct eigenvalues would require a decoupling network with 2(*k*–1) independent parameters. Decoupling of the array can be accomplished in *k*–1 stages by using a ladder of circulant symmetric network configurations (henceforth referred to as *stage networks*) which each consist of *N* identical series reactive elements followed by *N* identical parallel reactive elements. The parallel elements can be arranged in the shape of polygons (a single *N*-sided polygon or a set of smaller polygons rotated with respect to one another) or in the shape of a star (with or without a common node at the centre). We need to identify *k*–1 suitable stage networks. The stage networks will reduce to equivalent circuits resembling those in Fig. 1 for every eigenmode. We can determine the parameter *n* of a stage network for each mode by assuming port voltages corresponding to the appropriate eigenvector and using circuit analysis to obtain the equivalent network. Two modes with distinct eigenmode impedances can then be decoupled during each stage. After identifying the terminating impedance and the value of *n* for each of the two modes, the relations provided in (2) and (3) are used to determine the values of the series and parallel elements of the stage network. Note that the order in which the stage networks are employed is important. Once two modes have been decoupled, their equivalent networks should be identical for all subsequent stages in order to preserve the equality of their eigenmode impedances.

This principle is best illustrated by considering an example of a circulant symmetric 6-element array with elements regularly spaced on the circumference of a circle. For such an array, mutual coupling is only a function of the distance between elements, and therefore the scattering parameters of the array are given by

$$\mathbf{S^a} = \begin{bmatrix} S_{11}^a & S_{12}^a & S_{13}^a & S_{14}^a & S_{13}^a & S_{12}^a \\ S_{12}^a & S_{11}^a & S_{12}^a & S_{13}^a & S_{14}^a & S_{13}^a \\ S_{13}^a & S_{12}^a & S_{11}^a & S_{12}^a & S_{13}^a & S_{14}^a \\ S_{14}^a & S_{13}^a & S_{12}^a & S_{11}^a & S_{12}^a & S_{13}^a \\ S_{13}^a & S_{14}^a & S_{13}^a & S_{12}^a & S_{11}^a & S_{12}^a \\ S_{12}^a & S_{13}^a & S_{14}^a & S_{13}^a & S_{12}^a & S_{11}^a \end{bmatrix}. \tag{4}$$

The corresponding impedance matrix can be computed from

$$\mathbf{Z^a} = Z_0(\mathbf{I} + \mathbf{S^a})(\mathbf{I} - \mathbf{S^a})^{-1}, \tag{5}$$

where Z_0 is the characteristic impedance of the system. The eigenvalues of the impedance matrix (viz. the eigenmode impedances) are given by $Z_a = Z_{11}^a + 2Z_{12}^a + 2Z_{13}^a + Z_{14}^a$, $Z_b = Z_{11}^a - 2Z_{12}^a + 2Z_{13}^a - Z_{14}^a$, $Z_c = Z_d = Z_{11}^a - Z_{12}^a - Z_{13}^a + Z_{14}^a$ and $Z_e = Z_f = Z_{11}^a + Z_{12}^a - Z_{13}^a - Z_{14}^a$. The corresponding orthogonal eigenvectors are $\mathbf{e}_a = [1, 1, 1, 1, 1, 1]^T$, $\mathbf{e}_b = [1, -1, 1, -1, 1, -1]^T$, $\mathbf{e}_c = [1, 0, -1, 1, 0, -1]^T$, $\mathbf{e}_d = [1, -1, 0, 1, -1, 0]^T$, $\mathbf{e}_e = [1, 0, -1, -1, 0, 1]^T$ and $\mathbf{e}_f = [1, 1, 0, -1, -1, 0]^T$.

In order to decouple the array, we use a combination of the stage networks shown in Table I to equalize the eigenmode impedances. The equivalent circuit for each mode is defined in Fig. 2, while parameter *n* is specified in the second column of Table I. From Table I, it is clear that we can use the first network to decouple mode groups (*c* , *d*) and (*e* , *f*), the second network to decouple mode groups *b* and (*c* , *d* , *e* , *f*) and finally the third network for decoupling mode groups *a* and (*b* , *c* , *d* , *e* , *f*). The complete decoupling network is shown in Fig. 3.

Comparing the relevant equivalent circuits for mode groups (*c* , *d*) and (*e* , *f*) with those shown in Fig. 1, it follows that $X_1 = g(Z_c, Z_e)$ and $B_1 = h(Z_c, 3, Z_e, 1, X_1)$, with *g* and *h* as defined in (2) and (3). The new impedance parameters as seen from ports 1', 2', 3', 4', 5' and 6' in Fig. 3 are given by

$$\mathbf{Z}' = ((\mathbf{Z^a} + \mathbf{Z}_1)^{-1} + \mathbf{Y}_1)^{-1}. \tag{6}$$

The terms $\mathbf{Z}_1$ and $\mathbf{Y}_1$ in (6) are defined by

$$\mathbf{Z}_i = \mathrm{diag}[\,jX_i\,,\ jX_i\,,\ jX_i\,,\ jX_i\,,\ jX_i\,,\ jX_i\,], \tag{7}$$

and

$$\mathbf{Y}_1 = \begin{bmatrix} j2B_1 & -jB_1 & 0 & 0 & 0 & -jB_1 \\ -jB_1 & j2B_1 & -jB_1 & 0 & 0 & 0 \\ 0 & -jB_1 & j2B_1 & -jB_1 & 0 & 0 \\ 0 & 0 & -jB_1 & j2B_1 & -jB_1 & 0 \\ 0 & 0 & 0 & -jB_1 & j2B_1 & -jB_1 \\ -jB_1 & 0 & 0 & 0 & -jB_1 & j2B_1 \end{bmatrix}. \tag{8}$$

The eigenvalues for $\mathbf{Z}'$ are then obtained as $Z'_a = Z'_{11} + 2Z'_{12} + 2Z'_{13} + Z'_{14}$, $Z'_b = Z'_{11} - 2Z'_{12} + 2Z'_{13} - Z'_{14}$ and $Z'_c = Z'_d = Z'_e = Z'_f = Z'_{11} - Z'_{12} - Z'_{13} + Z'_{14}$. Note that modes *c*, *d*, *e* and *f* are now decoupled.

Subsequently, we decouple mode groups *b* and (*c* , *d* , *e* , *f*) using circuit elements X_2 and B_2. Comparing the equivalent circuits with those shown in Fig. 1 gives $X_2 = g(Z'_b, Z'_c)$ and $B_2 = h(Z'_b, 0, Z'_c, 3, X_2)$. The impedance parameters as seen from ports 1", 2", 3", 4", 5" and 6" in Fig. 3 are given by

$$\mathbf{Z}'' = ((\mathbf{Z}' + \mathbf{Z}_2)^{-1} + \mathbf{Y}_2)^{-1}, \tag{9}$$

where $\mathbf{Z}_2$ is defined by (7), and

$$\mathbf{Y}_2 = \begin{bmatrix} j2B_2 & 0 & -jB_2 & 0 & -jB_2 & 0 \\ 0 & j2B_2 & 0 & -jB_2 & 0 & -jB_2 \\ -jB_2 & 0 & j2B_2 & 0 & -jB_2 & 0 \\ 0 & -jB_2 & 0 & j2B_2 & 0 & -jB_2 \\ -jB_2 & 0 & -jB_2 & 0 & j2B_2 & 0 \\ 0 & -jB_2 & 0 & -jB_2 & 0 & j2B_2 \end{bmatrix}. \tag{10}$$

The eigenvalues of $\mathbf{Z}''$ are found as $Z''_a = Z''_{11} + 2Z''_{12} + 2Z''_{13} + Z''_{14}$ and $Z''_b = Z''_c = Z''_d = Z''_e = Z''_f = Z''_{11} - 2Z''_{12} + 2Z''_{13} - Z''_{14}$.

TABLE I
STAGE NETWORKS FOR MODE DECOUPLING.

Stage network	Parameter n in Fig. 2
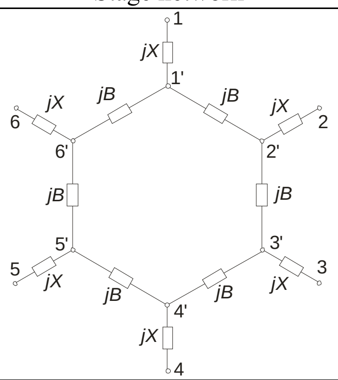	Mode a: $n = 0$ Mode b: $n = 4$ Modes c, d: $n = 3$ Modes e, f: $n = 1$
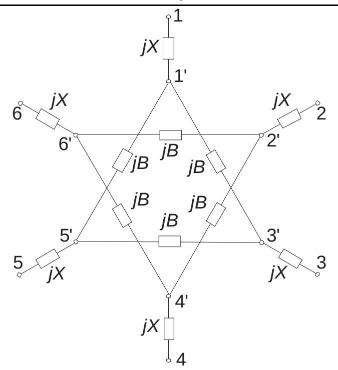	Modes a, b: $n = 0$ Modes c, d, e, f: $n = 3$
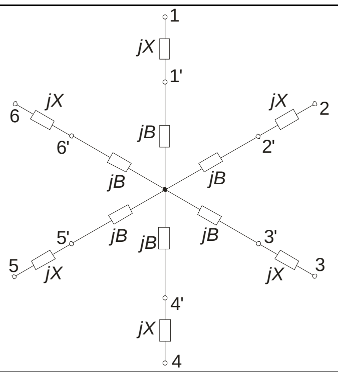	Mode a: $n = 0$ Modes b, c, d, e, f: $n = 1$

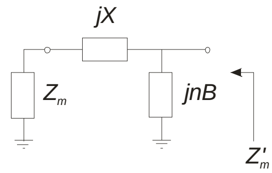

Fig. 2. Equivalent network of the stage networks shown in Table I when mode m is excited.

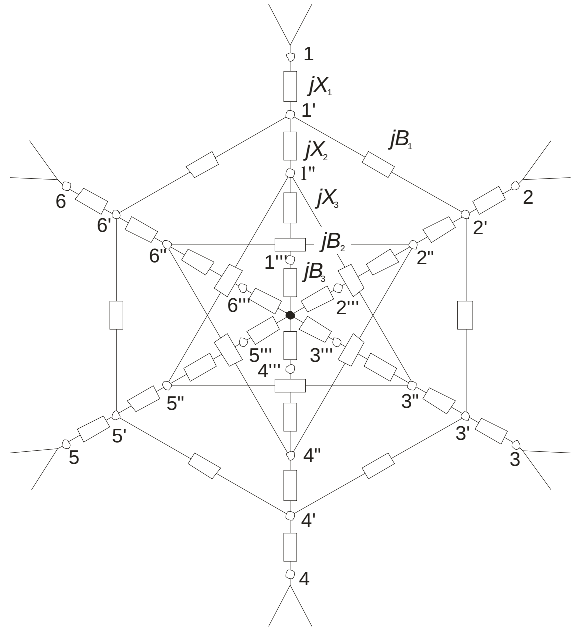

Fig. 3. Complete decoupling network for a symmetrical 6-element array.

Finally, mode groups a and (b, c, d, e, f) are decoupled. From the equivalent circuits for these modes, it follows that $X_3 = g(Z''_a, Z''_b)$ and $B_3 = h(Z''_a, 0, Z''_b, 1, X_3)$. The impedance parameters as seen from ports 1''', 2''', 3''', 4''', 5''' and 6''' are then given by

$$\mathbf{Z}''' = ((\mathbf{Z}'' + \mathbf{Z_3})^{-1} + \mathbf{Y_3})^{-1}, \tag{11}$$

where $\mathbf{Z_3}$ is defined by (7) and

$$\mathbf{Y_3} = \begin{bmatrix} j\frac{5}{6}B_3 & -\frac{j}{6}B_3 & -\frac{j}{6}B_3 & -\frac{j}{6}B_3 & -\frac{j}{6}B_3 & -\frac{j}{6}B_3 \\ -\frac{j}{6}B_3 & j\frac{5}{6}B_3 & -\frac{j}{6}B_3 & -\frac{j}{6}B_3 & -\frac{j}{6}B_3 & -\frac{j}{6}B_3 \\ -\frac{j}{6}B_3 & -\frac{j}{6}B_3 & j\frac{5}{6}B_3 & -\frac{j}{6}B_3 & -\frac{j}{6}B_3 & -\frac{j}{6}B_3 \\ -\frac{j}{6}B_3 & -\frac{j}{6}B_3 & -\frac{j}{6}B_3 & j\frac{5}{6}B_3 & -\frac{j}{6}B_3 & -\frac{j}{6}B_3 \\ -\frac{j}{6}B_3 & -\frac{j}{6}B_3 & -\frac{j}{6}B_3 & -\frac{j}{6}B_3 & j\frac{5}{6}B_3 & -\frac{j}{6}B_3 \\ -\frac{j}{6}B_3 & -\frac{j}{6}B_3 & -\frac{j}{6}B_3 & -\frac{j}{6}B_3 & -\frac{j}{6}B_3 & j\frac{5}{6}B_3 \end{bmatrix}. \tag{12}$$

All the modal impedances are then matched, since $Z'''_m = Z'''_{11}$, $m = a, b, \ldots f$. The new input ports will also be decoupled and will have the same input impedance. The ports can be matched to the system impedance Z_0 using L-section impedance matching networks [15].

To verify the theory, a decoupling network for a specific 6-element monopole array was designed and analyzed. The six elements of the array were evenly distributed on a circle with radius of 15mm (0.125λ at a center frequency of

$f_0 = 2.5$ GHz). Each monopole had a length of 28mm (0.23λ) and a diameter of 1mm (0.0083λ). With a system impedance of $Z_0 = 50\,\Omega$, the array's S-parameters were computed using IE3D [16] and converted into impedance parameters using (4). The scattering parameters of the array at f_0 and the computed decoupling network elements are specified in Table II. The elements of the L-section impedance matching networks are also shown, with B_4 being the susceptance of a parallel element to ground and X_4 the reactance of a series element. The scattering parameters were calculated over a frequency range of $0.98 f_0$ to $1.02 f_0$. The results shown in Fig. 4 clearly illustrate the validity of the theory.

TABLE II
SCATTERING PARAMETERS AND DECOUPLING NETWORK ELEMENTS FOR THE 6-ELEMENT ARRAY.

Array scattering parameters	$S_{11}^a = -6.79$ dB $\angle 159.3°$
	$S_{12}^a = -7.96$ dB $\angle 4.5°$
	$S_{13}^a = -15.33$ dB $\angle -53.4°$
	$S_{14}^a = -17.93$ dB $\angle -101.5°$
Decoupling network elements (Ω)	$X_1 = 4.4123$, $B_1 = 0.05184$
	$X_2 = -2.2399$, $B_2 = -0.06078$
	$X_3 = 2.7955$, $B_3 = 0.1087$
Decoupled port impedance (Ω)	$Z_{11}''' = 142.661 - j69.2205$
Matching network elements (Ω)	$B_4 = 0.006263$, $X_4 = 79.4505$

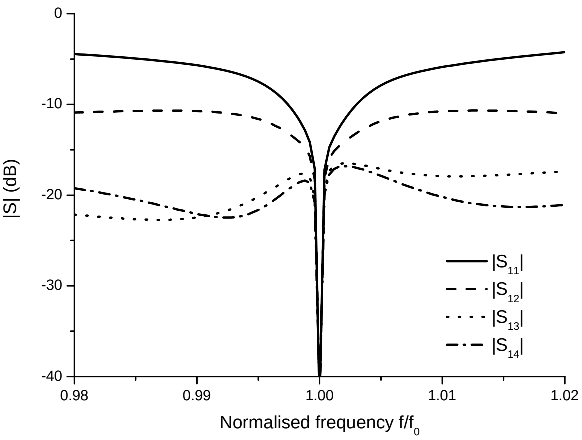

Fig. 4. Scattering parameters of the decoupled and matched 6-element array.

IV. CONCLUSION

We successfully demonstrated the design of a decoupling network for a circulant symmetric array with more than three elements. The bandwidth of the decoupled array is determined by the level of mutual coupling between array elements. Wideband impedance matching techniques cannot overcome this inherent limitation. It can only be alleviated by increasing the element spacing or using fewer elements.

When all input ports are decoupled and matched, no power fed into the system is reflected. Ideally, all this power should be radiated. In practice, significant power loss may occur in the decoupling and matching networks. These effects can be quantified by applying the procedure described in [13].

The principles presented in this paper provide a framework for the systematic design of decoupling networks for circulant symmetric arrays. The procedure is theoretically applicable to arrays of various sizes and has successfully been tested on arrays with up to 8 elements. However, due to the complexity of the circuit configuration, implementation of the decoupling network for a 6-element array would require the use of a multilayer circuit with at least three layers. Implementation would therefore be even more challenging for larger arrays.

REFERENCES

[1] J. H. Winters, J. Salz, and R.D. Gitlin, "The impact of antenna diversity on the capacity of wirelesscommunication systems", *IEEE Trans. Communications*, vol 42, no. 234, pp. 1740-1751, Feb./ Mar./ Apr. 1994.

[2] V. Jungnickel, V. Pohl and C. von Helmolt, "Capacity of MIMO systems with closely spaced antennas*", IEEE Communications Letters*, vol. 7, no. 8, pp. 361- 363, Aug. 2003.

[3] I.J. Gupta and A.A. Ksienski, "Effect of mutual coupling on the performance of adaptive arrays", *IEEE Trans. Antennas Propag.*, vol. AP-31, no. 5, pp. 785-791, Sept. 1983.

[4] H.J. Chaloupka and X. Wang, "Novel approach for diversity and MIMO antennas at small mobile platforms", in *Proc. IEEE Int. Symp. on Personal, Indoor and Mobile Radio Communications*, Barcelona, Spain, Sept. 2004, vol. 1, pp. 637- 642.

[5] J.B. Anderson and H.H. Rasmussen, "Decoupling and descattering networks for antennas*", IEEE Trans. Antennas Propag.*, vol. 24, no. 6, pp. 841-846, Nov. 1976.

[6] H.J. Chaloupka, X. Wang and J.C. Coetzee, "Performance enhancement of smart antennas with reduced element spacing", in *Proc. IEEE Conf. Wireless Communications and Networking*, vol. 1, pp. 425-430, Mar. 2003.

[7] H.J. Chaloupka, X. Wang and J.C. Coetzee, "Superdirective 3-element array for adaptive beamforming", *Microw. Opt. Technol. Lett.*, vol. 36, no. 6, pp. 425-430, Mar. 2003.

[8] P.T. Chua and J.C. Coetzee, "Microstrip decoupling networks for low-order multi-port arrays with reduced element spacing", *Microw. Opt. Technol. Lett.*, vol. 46, no. 6, pp. 592-597, Sept. 2005.

[9] H.J. Chaloupka, Y-H Lu and J.C. Coetzee, "A dual-polarized microstrip antenna array with port decoupling for MIMO systems", in *Proc. ISAP 2004*, Sendai, Japan, Aug. 2004, pp. 1229-1232.

[10] J. Weber, C. Volmer, K. Blau, R. Stephan, and M. A. Hein, "Miniaturized antenna arrays using decoupling networks with realistic elements" , *IEEE Trans. Microw. Theory Tech.*, vol. 54, no. 6, pp. 2733-2740, Jun. 2006.

[11] J.C. Coetzee and Y. Yu, "An alternative approach to decoupling of arrays with reduced element spacing", in *Proc. ISAP 2006*, Singapore, Nov. 2006.

[12] C. Volmer, J. Weber, R. Stephan, K. Blau and M.A. Hein, "Decoupling and matching network for miniaturised 3-port antenna arrays based on 180° couplers", in *Proc. Int. ITG Conf.*, Munich, Germany, March 2007, pp. 63-66.

[13] C. Volmer, J. Weber, R. Stephan, K. Blau and M.A. Hein, "An eigen-analysis of compact antenna arrays and its application to port decoupling", *IEEE Trans. Antennas Propag.*, vol. 56, no. 2, pp. 360-370, Feb. 2008.

[14] J.C. Coetzee and Y. Yu, "Port decoupling for small arrays by means of an eigenmode feed network*", IEEE Trans. Antennas Propag.*, vol. 56, no. 6, pp. 1587-1593, Jun. 2008.

[15] D.M. Pozar, *Microwave Engineering*, Hoboken: John Wiley & Sons, 2005, ch. 5.

[16] IE3D, Version 11.23, Zeland Software Inc., Fremont, 2006.